ELSEVIER

Journal of Nuclear Materials 249 (1997) 165–174

Atom probe characterization of the microstructure of nuclear pressure vessel surveillance materials after neutron irradiation and after annealing treatments

P. Pareige [a], R.E. Stoller [b], K.F. Russell [b], M.K. Miller [b,*]

[a] Laboratories de Microscopie Ionique, Faculte des Sciences et des Techniques, BP 118, 76134 Mont-Saint-Aignan cedex, France
[b] Metals and Ceramics Division, Oak Ridge National Laboratory, MS 6376, PO Box 2008, Oak Ridge, TN 37831-6376, USA

Received 18 February 1997; accepted 16 June 1997

Abstract

Microstructural changes due to neutron irradiation of weld and forging materials were characterized using the atom probe field ion microscope (APFIM). Neutron-induced clusters containing Cu, P, Ni, Mn and Si were detected in the high copper weld (0.24 at.% Cu) after irradiation to fluences of 6.6×10^{22} and 3.47×10^{23} $\mathrm{n\,m^{-2}}$; only phosphorus atmospheres were observed in the low copper forging material (0.02 at.% Cu) irradiated to an intermediate fluence of 1.5×10^{23} $\mathrm{n\,m^{-2}}$. These results are in agreement with previous studies and with their respective measured transition temperature shifts. In addition, APFIM experiments were carried out on the high fluence weld material after two post-irradiation annealing treatments. The first annealing treatment of 168 h at 454°C is similar to the proposed condition for in situ pressure vessel annealing and the second, 29 h at 610°C, is similar to the final stress relief heat treatment employed in vessel fabrication. Annealing at 454°C led to coarsening of the copper-enriched precipitates and a 92% recovery of the radiation-induced transition temperature shift. Essentially complete rehomogenization of the solutes was obtained in the simulated stress relief treatment at 610°C. © 1997 Elsevier Science B.V.

1. Introduction

The neutron irradiation-induced embrittlement of reactor pressure vessel (RPV) steels may lead to a reduction of the vessel service life. This behavior is now well established and is typically assessed by the measured increase in the ductile-to-brittle transition temperature (DBTT) of RPV materials. In addition to the need to maintain adequate safety margins for vessel operation the economic incentive associated with extending the lifetime of current RPVs has motivated research to identify embrittlement mechanisms and possible methods of mitigating embrittlement. Thermal annealing treatments have been identified as a suitable means to recover the mechanical properties. Recent studies of this thermal recovery, including in situ RPV anneals [1–5], have provided an extensive set of data describing the mechanical properties of irradiated, post-irradiation annealed, and reirradiated-annealed materials. Although the mechanical behavior of these materials is relatively well-known, little information is available as far as microstructural changes are concerned.

The extremely small size, up to few nm, of the features that evolve in the microstructure under neutron irradiation and after annealing treatments make atom probe field ion microscopy (APFIM) [6] one of the most suitable techniques for resolving outstanding questions in this field of research. Therefore, an APFIM investigation of the microstructure of commercial reactor pressure vessel steels in the as-irradiated (AI) and post-irradiation annealed (PIA) conditions was performed. The experiments described in this paper were performed in the Oak Ridge National Laboratory (ORNL) energy-compensated instrument [7].

The degree of radiation-induced embrittlement in RPV steels is known to be quite sensitive to copper content,

* Corresponding author. Tel.: +1-423 576 7886; fax: +1-423 574 0641; e-mail: rkn@ornl.gov.

PII S0022-3115(97)00215-8

even for bulk levels as low as 0.09 wt% [8]. For this reason, two types of material from the Babcock & Wilcox Master Integrated Reactor Vessel Surveillance Program were investigated. The first was a SA-508, class 2 forging steel, with a nominal copper content of 0.02 wt%. The second material was a typical Mn–Mo–Ni-weld wire/Linde 80 flux submerged arc weld, representative of the materials used to fabricate the beltline shell course regions of the Oconee Unit-3 and Arkansas Unit-1 RPV. The nominal copper level in this weld is ~ 0.3 wt%, or 15 times higher than in the forging. The experimental results we obtained show that the neutron irradiation had a negligible influence on the microstructure of the forging material, whereas extensive changes were observed in the weld. Because of these initial observations, only the irradiated weld specimens were heat treated for the study of annealing effects.

In order to isolate the effect of the neutron irradiation, these materials were previously characterized in the as-received (i.e., as stress relieved) and long-term thermally aged (i.e., stress relieved + 100000 h at 280°C) conditions. A detailed description of these results can be found in Ref. [9]. The most important conclusion from this study was that long-term thermal-aging at 280°C appeared to have no influence on the microstructure. This lack of microstructural evolution was consistent with the mechanical properties reported in Ref. [10].

2. Materials and experimental

The bulk composition of the forging and weld materials used in this study is given in Table 1. For purposes of comparison, the compositions are shown in both atomic and weight percent. Subsequent APFIM compositions are all reported in atomic percent. The forging material was austenetized at 854–877°C for 4 h and water quenched, then tempered at 666–688°C for 10 h and water quenched and finally stress relieved at 593–621°C for 30 h and furnace cooled. The weld material was subjected to a stress relief heat treatment for 29 h at 593–621°C and furnace cooled at a rate of ~ 8°C/h to ~ 310°C. The composition of the ferrite matrix of the as-received materials was also obtained as part of a previous study using the same APFIM technique. These reference compositions are summarized in Tables 2 and 3 along with the compositions measured in the various irradiated conditions.

The weld material was irradiated to both a low and a high fluence and the forging material to an intermediate fluence. The irradiation conditions (flux, fluence and temperature) and the associated increase of 41J Charpy transition temperature due to neutron irradiation of these materials are reported in Table 4 [10–12]. The APFIM samples ($0.3 \times 0.3 \times 20$ mm^3) were cut from broken Charpy V-notch specimens.

It should be noted from Tables 1 and 3, that the matrix copper content of the weld material is depleted from the bulk level of 0.24 to 0.14 at.% after the stress relief heat treatment. This lower value is in agreement with the predicted solubility limit of the SGTE database [13] for the FeCu binary system for the given temperature of the stress relief heat treatment and a slow furnace cool. The observed depletion in Mn, C, Mo and Cr elements can be accounted for by the presence of M_3C cementite-type and Mo_2C-type carbides which are enriched in these elements.

The annealing treatment selected for the weld material was based on a previous study investigating the effects of annealing time and temperature on the recovery of Charpy V-notch properties of irradiated high copper weld metal [3]. This study showed that a reasonable compromise between the highest degree of recovery and an acceptable annealing time at a technically achievable temperature is 168 h at 454°C. Thus, four APFIM bars of the weld material at the highest fluence of 3.47×10^{23} n m^{-2} were encapsulated in quartz tubes and annealed for 168 h at 454°C. In addition to these specimens, four others were encapsulated and annealed for 29 h at 610°C, which was the initial stress relief heat treatment. Both capsules were furnace cooled.

Both field ion microscopy and atom probe experiments were performed. The experimental conditions used for the analyses included a pulse fraction of 20% and a specimen temperature of 50 K to avoid a systematic error in the copper level measurement [14]. Field ion needles were electropolished using standard procedures [6]. All compositions reported in this paper are quoted in atomic percent. Concentration uncertainties (2σ) for each element due to counting errors are given by the standard deviation $\sigma = [X(1-X)/N]^{1/2}$, where N is the total number of atoms

Table 1
Chemical composition (bulk chemistry) of forging and weld surveillance materials (balance is iron)

		Cu	Ni	Mn	Si	P	C	S	Mo	Cr
Forging	wt%	0.02	0.76	0.72	0.21	0.014	0.24	0.012	0.62	0.34
	at.%	0.017	0.72	0.72	0.41	0.025	1.11	0.021	0.36	0.36
Weld	wt%	0.28	0.59	1.49	0.51	0.016	0.09	0.016	0.39	0.06
	at.%	0.24	0.56	1.5	1.01	0.03	0.42	0.03	0.23	0.06

Table 2
Composition (APFIM data) of the ferrite matrix of the forging material in various conditions (balance is iron)

	at.% $\pm 2\sigma$							
	Cu	Ni	Mn	Si	P	C	Mo	Cr
Bulk	0.017	0.72	0.72	0.41	0.025	1.11	0.36	0.36
Reference (as-stress-relieved)	0.03 ± 0.01	0.72 ± 0.07	0.48 ± 0.06	0.50 ± 0.06	0.02 ± 0.01	0.004 ± 0.004	0.12 ± 0.03	0.15 ± 0.03
Neutron irradiated fluence: 1.45×10^{23} n m^{-2}	0.02 ± 0.02	0.70 ± 0.10	0.54 ± 0.09	0.52 ± 0.09	0.003 ± 0.003	0.02 ± 0.02	0.07 ± 0.03	0.19 ± 0.05

collected and X is the fraction of those atoms that are of the given element.

3. Results and discussion

The results are presented in two parts. First, the results obtained on the neutron irradiated weld and forging materials will be discussed. Since the ferrite matrix is supersaturated with certain solutes at the irradiation temperature, the matrix chemistry was analyzed for each material condition. The APFIM analysis also focused on characterizing the density and chemical content of the radiation-induced defect/solute clusters that were detected. Then, a similar microstructural characterization of the neutron-irradiated and annealed weld metal will be described.

3.1. Neutron irradiated forging and weld

3.1.1. Irradiated weld

Samples of weld metal which had been exposed to a low and a high neutron fluence, 6.6×10^{22} and 3.47×10^{23} n m^{-2} ($E > 1$ MeV), were studied using the atom probe field ion microscope. The results on the matrix measurements are summarized in Table 3. The bulk chemistry, as well as the as-received reference value are listed for comparison.

These results show that the neutron irradiation has further reduced the matrix copper level beyond the depletion which occurred during the stress relief treatment. The depletion is more pronounced at the highest dose. The copper depletion of the matrix is also associated with a phosphorus depletion for both irradiation conditions. The difference between the phosphorus contents measured at the two fluences is not statistically significant. Other solute contents (except for Cr) are consistent with the composition expected to result from the initial heat treatment. It must be noted that compositions are, in each case, an average of several experiments. These RPV steels can exhibit significant compositional variation in APFIM measurements since only a small volume of material ($\sim 3 \times 10^{-25}$ m^3) is sampled from any given specimen.

Although the matrix chemistry changes were modest, a high number density ($\sim 10^{23}$ and $\sim 3 \times 10^{23}$ m^{-3} after fluences of 6.6×10^{22} and 3.47×10^{23} n m^{-2} respectively) of ultra-fine (2–3 nm in diameter) solute clusters were observed and analyzed. These intragranular clusters were enriched in Cu, P, Ni, Mn and Si. A representative composition profile through one of the copper-enriched clusters is shown in Fig. 1. The size and composition of these copper-enriched clusters were similar at low and high fluence. The average composition of these copper-enriched clusters and their enrichment factors (defined as the ratio of the solute concentration detected in the cluster to the concentration measured in the matrix), are reported in Table 5.

Table 3
Composition (APFIM data) of the ferrite matrix of the weld material in various conditions

	at.% $\pm 2\sigma$							
	Cu	Ni	Mn	Si	P	C	Mo	Cr
Bulk	0.24	0.56	1.50	1.01	0.03	0.42	0.23	0.06
Reference (as-stress-received)	0.14 ± 0.03	0.45 ± 0.06	1.20 ± 0.10	1.05 ± 0.10	0.03 ± 0.03	0.005 ± 0.005	0.18 ± 0.04	0.03 ± 0.03
Low fluence 6.6×10^{22} n m^{-2}	0.13 ± 0.04	0.61 ± 0.08	1.54 ± 0.14	0.75 ± 0.10	0.003 ± 0.003	0.01 ± 0.01	0.17 ± 0.04	0.09 ± 0.03
High fluence 3.5×10^{23} n m^{-2}	0.05 ± 0.01	0.57 ± 0.05	1.08 ± 0.07	1.22 ± 0.07	0.013 ± 0.007	0.005 ± 0.005	0.23 ± 0.03	0.08 ± 0.02

Table 4
Irradiation conditions of the forging and the weld materials and their respective transition temperatures

Material	Plant	Average flux (10^{14} n m^{-2} s^{-1})	Fluence (10^{23} n m^{-2}) ($E > 1$ MeV)	Irradiation temperature (°C)	ΔT_{41J} (°C)
Forging	Oconnee-3	2.5–6.6	1.45	288	31 [10]
Weld	Rancho-Seco	3.6–10	0.66	292	84 [11]
	Pt-Beach-2	7.4	3.47	283	128 [12]

A detailed and accurate description of one of these neutron-induced copper-enriched clusters provided by an atomic-plane-by-plane-type analysis [6] is reported in Ref. [15]. A very high enrichment is observed for copper and phosphorus and a less, but significant, enrichment is also observed for nickel, manganese and silicon solutes. Concentrations of manganese and nickel appear to be essentially equal in all of the clusters that have been analyzed. The presence of these small copper-enriched clusters in these irradiated materials is consistent with the measured increase in the ductile-to-brittle transition temperature. As reported in Table 4, the temperature shifts are 84 and 128°C for materials irradiated to 6.6×10^{22} and 3.47×10^{23} n m^{-2}, respectively. The fact that the clusters detected in this study were not observed in the reference and the long-term thermally-aged materials confirms that their formation is either irradiation-induced or irradiation-enhanced.

It must be noted, as has been previously reported in the case of a French pressure vessel steel (Chooz A) [16,17], that only the number density of the copper-enriched clusters was found to increase with fluence. The average cluster size was similar at both fluences. The main difference between the neutron-induced clusters observed in the French steel and in the US weld examined in this study is their copper contents. The measured copper contents appear consistent with the respective residual copper levels prior to irradiation, 0.08 at.% for Chooz A and 0.14 at.% for the US weld. However, the results of a small angle neutron scattering (SANS) study of an RPV steel with a somewhat higher copper level has found different results [18]. The authors of the SANS study reported that the density of copper-enriched clusters decreased and the average radius increased as the neutron fluence increased. The altered fluence dependence could be due to compositional differences between the alloys examined or an unresolved interpretive difference between the two experimental techniques.

The solute cluster densities from this study have been compared with a compilation of data from the literature that was reported in Ref. [16]. This compilation of cluster densities for various irradiation conditions is summarized in Table 6 [17,19,20,22]. These same data are also plotted

Table 5
Mean composition and associated enrichment factors of the copper enriched clusters detected in the neutron irradiated weld material

Fluence (n m^{-2})		Cu	P	Ni	Mn	Si	Cr	Mo	Fe
6.6×10^{22}	at.%	7.8	1.2	4.2	4.9	1.5	–	0.5	71.5
	enr. factor	60	400	6.9	3.2	2	–	3	–
3.5×10^{23}	at.%	5.8	0.4	5.1	5.2	2.9	0.1	0.3	80.6
	enr. factor	116	31	9	5	2	1.3	1.4	–

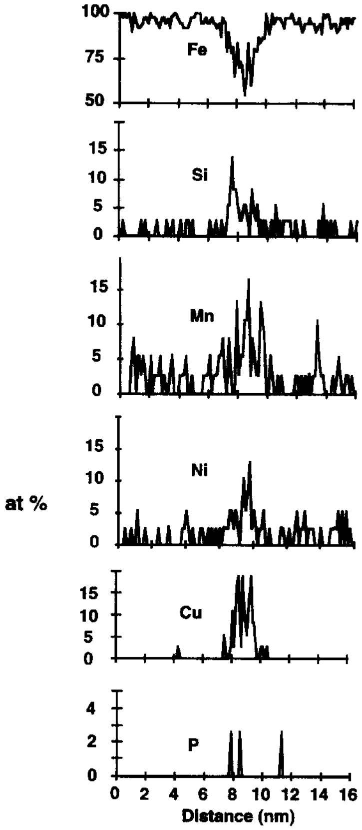

Fig. 1. Composition profile of a cluster analyzed in the weld material after neutron irradiation to 3.5×10^{23} n·m^{-2}, ($E > 1$ MeV).

in Fig. 2. The line drawn through the data points is a simple power law with the coefficients indicated on the figure. It must be noted that data are limited, for purposes of comparison, to materials having a low ferrite copper content (i.e., < 0.15 wt%) prior to irradiation.

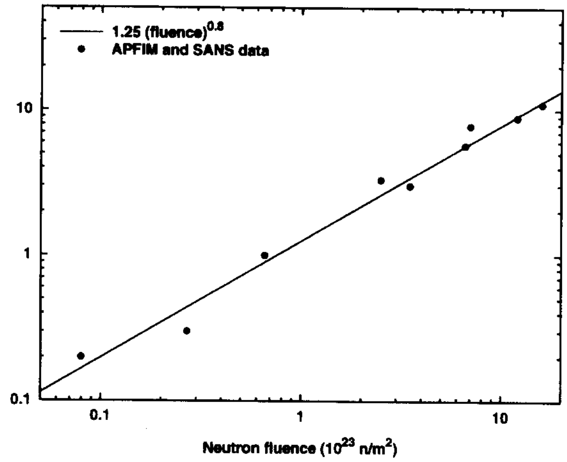

Fig. 2. Fluence dependence of copper-enriched solute clusters density obtained by APFIM and SANS (see Table 6).

Table 6 and Fig. 2 indicate that the cluster number density consistently increases as the neutron fluence increases. The evolution of radiation-induced solute clusters appears to proceed in a similar manner in all these materials.

3.1.2. Irradiated forging

The measured ferrite matrix composition of the irradiated forging material at a fluence of 1.45×10^{23} n m^{-2} is given in Table 2. The bulk chemistry and the reference as-received state are also reported for comparison. The large uncertainties associated with the reported concentrations are due to the low number of ions collected during experiments. This is due to the limited number of specimens available for this type of material. However, within the two-sigma uncertainty limit, the solute concentrations in the irradiated material are similar to the as-received

Table 6
Comparison of the copper content in the ferrite matrix of neutron irradiated steels

Ref.	Steel	Fluence (n m^{-2})	Flux (n/m^2/s)	Matrix copper content (at.%)		Cluster density (10^{23} m^{-3})
				unirradiated	irradiated	
[22]	A533-B	2×10^{21}		0.13	0.10 ± 0.03	
[19]	KRB-A	8.4×10^{21}	8.8×10^{16}	0.14	0.13	0.2
[19]	KRB-A	2×10^{22}		0.14	0.12	
[22]	KRB-A	2.7×10^{22}	8.5×10^{16}	0.14	0.11 ± 0.01	0.3
[16]	CHOOZ	4.7×10^{22}		0.08	0.05 ± 0.01	
This study	WELD	6.6×10^{22}	$\sim 7 \times 10^{15}$	0.14	0.13 ± 0.04	1.0
[22]	KRB-A	8.5×10^{22}		0.14	0.09 ± 0.01	
[16,17]	CHOOZ	2.5×10^{23}	$\sim 1 \times 10^{15}$	0.08	0.04 ± 0.01	3.3
This study	WELD	3.5×10^{23}	$\sim 7 \times 10^{15}$	0.14	0.05 ± 0.01	3.0
[16,17]	CHOOZ	6.6×10^{23}	$\sim 1 \times 10^{15}$	0.08	0.03 ± 0.04	5.7
[20]	SA-508	7.0×10^{23}	5×10^{16}	0.06		7.8
[16,17]	CHOOZ	1.2×10^{24}	$\sim 1 \times 10^{15}$	0.08	0.04 ± 0.01	8.9
[17]	CHOOZ	1.6×10^{24}	$\sim 1 \times 10^{15}$	0.08		11

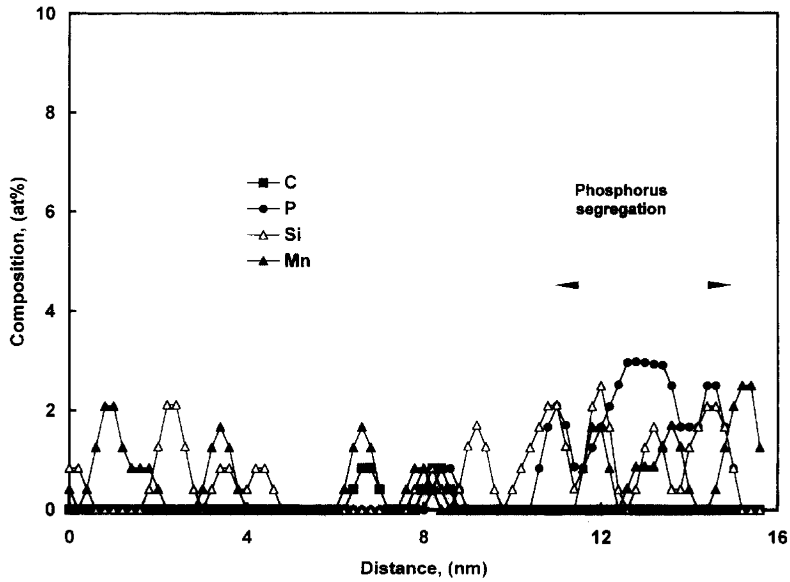

Fig. 3. Composition profile of an intragranular phosphorus atmosphere detected in the ferrite matrix of the forging material after neutron irradiation fluence to 1.45×10^{23} n m^{-2}.

material. The exceptions are phosphorus which is depleted and carbon which is slightly enhanced as the irradiation proceeds. The matrix carbon content is much lower than the bulk chemistry due to carbide precipitation.

A careful examination of atom probe composition profiles from the irradiated forging did not reveal the presence of copper clusters as they were observed in the irradiated weld. This absence of copper clusters is in good agreement with the detected copper level in the matrix. However, because of the small volume of material examined, it cannot be concluded that copper clusters are completely non-existent. If the number density of clusters is less than $\sim 10^{22}$ m^{-3}, the probability of encountering one during an atom probe analysis would be quite low.

The only detectable microstructural changes that have been observed in the ferrite matrix of the forging material were intragranular phosphorus atmospheres. A typical composition profile is shown in Fig. 3. The solute concentrations (in at.%) and their respective enrichment factors (shown in brackets), in these phosphorus atmospheres were P: 1.8 ± 0.9 (600), C: 0.1 ± 0.1 (5), Si: 1.2 ± 0.8 (2.3), Mo: 0.1 ± 0.1 (1.4), Mn: 0.7 ± 0.6 (1.3). The high phosphorus level in these atmospheres is consistent with its observed depletion in the matrix. These phosphorus-enriched regions are similar to those previously observed in APFIM studies of model [21] and commercial [22] pressure vessel steels.

3.1.3. Discussion

As shown in Table 6, the number of neutron-induced clusters detected in the matrix increased with the neutron fluence. A similar comparison can be made between the evolution of the copper content of the ferritic matrix and the accumulated neutron fluence. The respective matrix copper levels prior to and following irradiation are also listed in Table 6 [16,19,22]. These same data are plotted in Fig. 4, where the ratio of the copper content at a given fluence has been divided by the initial matrix copper content.

The values in Table 6 indicate that there is a rapid copper depletion during the first years of irradiation and that the copper level appears to saturate at a value of about 0.03–0.04 at.%. Three other results concerning the neutron-irradiated Fe–Cu binary system can be compared to

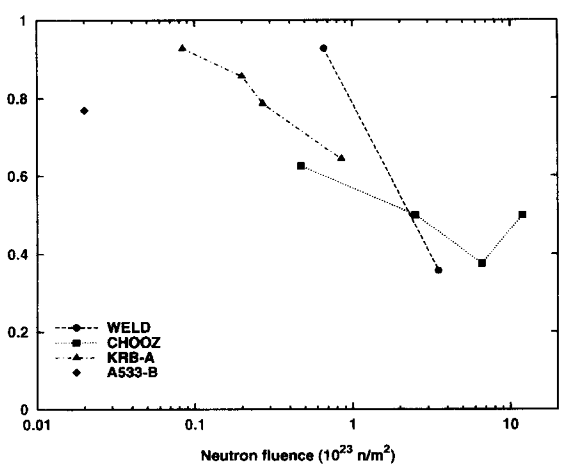

Fig. 4. Fluence dependence of the matrix copper content normalized by the initial matrix copper content for several steels. See Table 6 for explanation of symbols.

Table 7
Weld metal ferrite matrix composition in the as-stress-relieved, as-irradiated, and two post-irradiation-annealed conditions

	at.% $\pm 2\sigma$							
	Cu	Ni	Mn	Si	P	C	Mo	Cr
As-stress-relieved	0.14±0.03	0.45±0.06	1.20±0.06	1.05±0.10	0.03±0.02	0.005±0.005	0.18±0.04	0.03±0.02
Neutron irradiated (3.5×10^{23} n m^{-2})	0.05±0.01	0.57±0.05	1.08±0.07	1.22±0.07	0.013±0.007	0.005±0.005	0.23±0.03	0.08±0.02
Neutron irradiated and annealed (168 h at 454°C)	0.04±0.02	0.51±0.06	1.10±0.09	1.10±0.09	0.03±0.01	0.04±0.02	0.18±0.04	0.05±0.02
Neutron irradiated and annealed (29 h at 610°C)	0.17±0.04	0.58±0.07	0.85±0.08	0.90±0.09	0.01±0.01	0.01±0.01	0.17±0.04	0.05±0.02

the values in Table 6. These results are: Fe–0.13 at.% Cu at a fluence of 1.2×10^{23} n m^{-2}, matrix copper content = 0.05 ± 0.01 at.% [13]; Fe–0.09 at.% Cu, fluence = 5.5×10^{23} n m^{-2}, matrix copper = 0.03 ± 0.01 at.% [17] and Fe–0.17 at.% Cu, fluence = 5.5×10^{23} n m^{-2}, matrix copper = 0.03 ± 0.01 at.% [17].

All these experiments in commercial materials or the Fe–Cu binary system indicate that after high fluence neutron irradiation the copper content in the ferrite matrix is depleted to approximately 0.03–0.04 at.%. This observation suggests that such a value represents the quasi-equilibrium concentration under irradiation and could explain why no copper clusters were observed in the neutron-irradiated forging material which had a bulk copper content of 0.02 at.%.

3.2. Influence of the annealing heat treatment on neutron-irradiated weld material

The interest in post irradiation annealing arises from the fact that some early nuclear power reactor pressure vessels were fabricated in such a way that they may not meet some pertinent regulatory requirements as they near end-of-life. For example, predictions suggest that several vessels may exceed the DBTT limits set by regulations concerned with pressurized-thermal shock [23]. For such reactors, thermal annealing may be performed to mitigate the effects of neutron embrittlement. Recently, an investigation of the annealing response of an irradiated high copper submerged arc weld HSSI 73 W (HSSI: heavy steel irradiation) was performed [3]. This weld is similar to the weld examined in this study. The main differences in the bulk composition are: P: 0.005 wt% (73W)–0.016 wt% (this study), S: 0.005 wt% (73W)–0.016 wt% (this study), Mo: 0.58 wt% (73W)–0.39 wt% (this study), Cr: 0.25 wt% (73W)–0.06 wt% (this study). It was reported that annealing at 454°C for 24 h recovered about two-thirds of the transition temperature shift caused by the neutron irradiation. Annealing at this temperature for longer times increases the recovery, but at a decreasing rate, so that doubling the annealing time from 168 to 336 h increases the recovery from 92 to 96%.

Based on this experience, the high-fluence neutron-irradiated (3.5×10^{23} n m^{-2}) weld material of this study was annealed for 168 h at 454°C. The microstructural characterization of this annealed material is of prime interest, primarily to understand how recovery takes place, but also to give information on how the microstructure could evolve after re-irradiation. In addition to this standard annealing treatment, an annealing treatment was performed which corresponds to the initial stress relief heat treatment condition, i.e., 29 h at 610°C.

3.2.1. Annealing 168 h at 454°C

The ferrite matrix composition of the annealed weld material is reported in Table 7. The composition of the

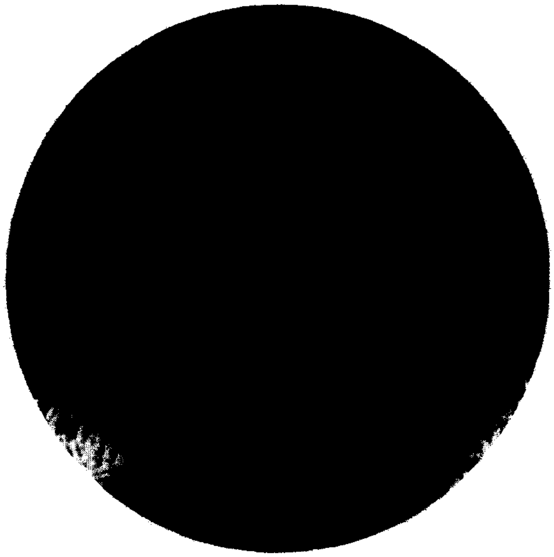

Fig. 5. Field ion micrograph of the ferrite matrix of the neutron-irradiated (3.5×10^{23} n·m^{-2}, $E > 1$ MeV) and annealed (168 h at 454°C) weld material. The dark area (arrow) is the field ion image of a copper precipitate (diameter ~ 5 nm). The dark disk in the middle of the image is entrance aperture to the mass spectrometer.

as-stress-relieved and as-irradiated material is also reported for comparison. These results show that there are no significant changes in the matrix composition due to the annealing. The copper matrix content is still depleted to about 0.04 at.%, similar to that observed after neutron irradiation. Only phosphorus and carbon are detected at higher levels (2.3 and 8 times, respectively) after the annealing treatment. Other solute contents remain essentially constant before and after annealing. However, none of the neutron-induced solute clusters described previously were detected in the annealed material. This implies that they either all dissolved during the heat treatment, or their number density decreased so much that they were not detected with the atom probe technique. In order to answer the question of how the copper had been redistributed, several additional specimens were observed using the field ion microscope (FIM). This permits the observation of the atomic plane by atomic plane evaporation of a large volume of the material to be achieved. The volume examined was about a hundred times more than the volume sampled with the atom probe.

One of the FIM experiments revealed the presence of a small dark-contrast area, shown in Fig. 5, which is characteristic of a copper precipitate [24]. The size of this precipitate was estimated to be on the order of 5 nm. Unfortunately, only a small portion of this precipitate could be analyzed with the atom probe since the precipitate had been partially field evaporated during FIM observation. The selected area analysis of the remaining portion of the dark area gave the composition profile shown in Fig. 6. This experiment and the associated composition profile do not provide quantitative information on the precipitate composition. First, because only a small portion of the precipitate was analyzed and secondly because a quantitative composition is reliable only when it has been measured several times in different precipitates. Although only one of these precipitates was observed, the composition profile indicates that the copper content is at least 60%.

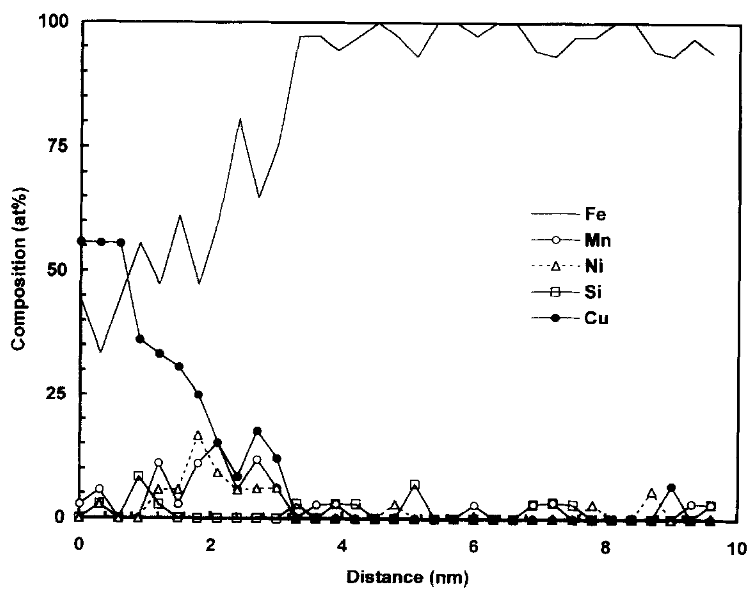

Fig. 6. Composition profile through a portion of the copper cluster observed in Fig. 3, in the ferrite matrix of the neutron-irradiated (3.5×10^{23} n m^{-2}, $E > 1$ MeV) and annealed (168 h at 454°C) weld material.

In addition, an enrichment of Ni and Mn solutes was observed at the interface in Fig. 6. Such enhancement of Ni solute at the interface of a growing copper precipitate is in good agreement with previous studies on a Fe–1.28 wt% Cu–1.43 wt% Ni ternary alloy [25]. This could be explained by the rejection of some solute atoms in the core of the particle towards the interface during the growth process of a nearly pure copper precipitate. The observation of this large copper precipitate may explain why the matrix is still copper-depleted despite the disappearance of the small neutron-induced clusters. In addition, the large amount of copper detected in this particle is in good agreement with the fact that the particle number density appears to be very low (only one of these was detected in this study). Assuming that these large copper precipitates (5 nm in diameter) are from 60 to 100% pure copper, the results of this study indicate that the precipitate number density would be in the range of 1.5 to 2.5×10^{22} m^{-3}. Moreover, it should be noted that the detected copper level in the matrix is exactly equal to the copper solubility limit given by the SGTE database [13] for a temperature of 450°C.

3.2.2. Annealing 29 h at 610°C

As expected from this heat treatment, the ferrite matrix composition is similar to the as-stress-relieved condition (this is shown in Table 7). Notably, the copper content has increased from 0.05 ± 0.01 to 0.17 ± 0.04 at.% which suggests that all the intragranular neutron-induced copper clusters have dissolved. The evolution of the copper content in the weld material after stress-relief heat-treatment, neutron irradiation and both annealing treatments is schematically shown in Fig. 7. Fig. 7 illustrates the loss of copper from the matrix due to precipitation during the initial stress relief, and the subsequent loss due to radiation-induced precipitation at ~ 290°C. The effect of the two PIA treatments is also shown.

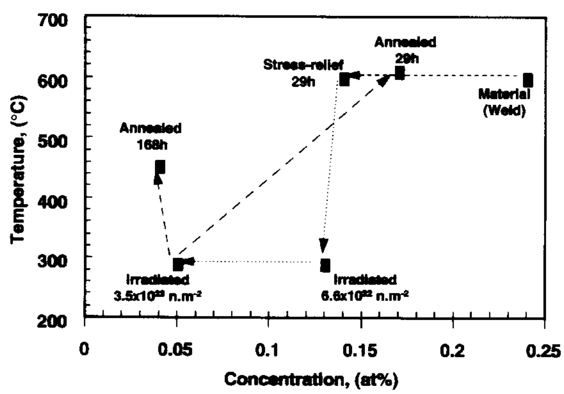

Fig. 7. Influence of neutron irradiation and annealing on the copper content of the matrix in a weld material.

4. Conclusion

Microstructural characterization of neutron-irradiated surveillance materials obtained from the B&W Owners Group was performed. Both an intermediate-copper level weld and a low-copper forging material were investigated. The maximum neutron fluence of the materials was 3.5×10^{23} $n\,m^{-2}$ ($E > 1$ MeV). The irradiated weld was also examined after two post-irradiation heat treatments: 168 h at 454°C and 29 h at 610°C.

Atom probe investigations have demonstrated a significant level of copper and phosphorus depletion in the neutron-irradiated weld ferrite matrix. In addition, a high number density of ultrafine intragranular clusters containing Cu, P, Ni, Mn and Si were observed and analyzed in this material. The copper concentration in the matrix of this weld after neutron irradiation is determined to be as low as 0.05 ± 0.01 at.%. This value is in good agreement with previous results available in the literature concerning high-fluence neutron-irradiated reactor pressure vessel steels. This result is also in agreement with the fact that no copper clusters were detected in the forging material (low copper level: 0.02 at.%) after irradiation to a neutron fluence of 1.45×10^{23} $n\,m^{-2}$. Only phosphorus atmospheres were detected as an effect of the irradiation in this low copper surveillance material.

The results concerning the annealing treatment performed on the high-fluence neutron irradiated weld material indicate that the neutron-induced copper clusters evolve by an Ostwald ripening process. The smallest clusters dissolve and the growth of larger copper particles takes place. After 168 h at 454°C, the copper concentration in the matrix is of the order of 0.04 ± 0.01 at.% which is in agreement with the copper solubility limit at this temperature.

The presence of neutron-induced copper clusters after neutron irradiation is in agreement the measured transition temperature shift. Also, their dissolution after annealing is in agreement with the high percentage of recovery. This indicates that the low number density of copper particles in the ferrite matrix after annealing has little influence on the mechanical properties of the recovered weld material.

Finally, it should be noted that if an annealing treatment leads to a low number density of small, nearly pure copper particles and a low matrix copper content, further neutron irradiation of this neutron-irradiated and annealed material should not produce large transition temperature shifts. This projection assumes that radiation-induced copper clusters are primarily responsible for the shift in the DBTT following neutron irradiation.

Acknowledgements

The materials for this study were provided by the B&W Owners Group. The authors would like to thank M.

J. De Van and W.A. Pavinich of B & W Nuclear Technologies and M.A. Sokolov of Oak Ridge National Laboratory for their assistance. This research was sponsored by the Division of Materials Sciences, US Department of Energy, under contract DE-AC05-96OR22464 with Lockheed Martin Energy Research Corp. and by the Office of Nuclear Regulatory Research, US Nuclear Regulatory Commission under inter-agency agreement DOE 1886-8109-8L with the US Department of Energy. This research was conducted utilizing the Shared Research Equipment (SHaRE) User Program facilities at Oak Ridge National Laboratory.

References

[1] A.D. Amayev, A.M. Kryukov, M.A. Sokolov, in: Radiation Embrittlement of Nuclear Reactor Pressure Vessel Steels: An International Review, Vol. 4, ASTM STP 1170, ed. E. Lendell Steele (American Society for Testing and Materials, Philadelphia, PA, 1993) p. 369.

[2] A.M. Kryukov, M.A. Sokolov, in: Small Specimen Test Techniques Applied to Nuclear Reactor Vessel Thermal Annealing and Plant Life Extension, ASTM STP 1204, eds. W.R. Corwin, F.M. Haggag and W.L. Server (American Society for Testing and Materials, Philadelphia, PA, 1993) p. 417.

[3] S.K. Iskander, M.A. Sokolov, R.K. Nanstad, in: Effects of Radiation on Materials: 17th Int. Symp., ASM STP 1270, eds. A.S. Kumar, D.S. Gelles, R.K. Nanstad and E.A. Little (American Society for Testing and Materials, Philadelphia, PA, 1994) p. 277.

[4] E.D. Eason, J.E. Wright, E.E. Nelson, G.R. Odette, E.V. Mader, Models for Embrittlement Recovery Due to Annealing of Reactor Pressure Vessel Steels, NUREG/CR-6327, MCS 950302 (Modeling and Computing Services, Boulder, CO, 1995).

[5] J.R. Hawthorne, A.L. Hiser, in: Environmental Degradation of Materials in Nuclear Power Systems: Water Reactors, Fifth Int. (American Nuclear Society, LaGrange Park, IL, 1991) p. 671.

[6] M.K. Miller, G.D.W. Smith, Atom Probe Microanalysis: Principles and Applications to Materials Problems (Materials Research Society, Pittsburgh, PA, 1989).

[7] M.K. Miller, J. Phys. (Paris) 47C2 (1986) 493.

[8] P. Pareige, J.C. Van Duysen, P. Auger, Appl. Surf. Sci. 67 (1993) 342.

[9] P. Pareige, K.F. Russell, R.E. Stoller, M.K. Miller, submitted to J. Nucl. Mater.

[10] M.J. DeVan, A.L. Lowe, C.S. Wade, in: Effects of Radiation on Materials: 16th Int. Symp., ASTM STP 1175, eds. A.S. Kumar, D.S. Gelles, R.K. Nanstad and E.A. Little (American Society for Testing and Materials, Philadelphia, PA, 1993) p. 268.

[11] A.L. Lowe et al., Analysis of Capsule RS1-D, Sacramento Municipal Utility District, Rancho-Seco Unit 1, BAW 1792, Babcock and Wilcox Co, Lynchburg, VA, Oct. 1983.

[12] A.L. Lowe et al., Analysis of Capsule S, Wisconsin Electric Power Co., Point Beach Unit 2 Reactor Material Surveillance Program, BAW 2140, B&W Nuclear Technologies, Lynchburg, VA, Aug. 1991.

[13] M.K. Miller, K.F. Russell, A. Jostons, R.G. Blake, Appl. Surf. Sci. 87&88 (1995) 216.

[14] G.M. Worrall, G.D.W. Smith, J. Phys. (Paris) 47C2 (1986) 245.

[15] P. Pareige, M.K. Miller, Appl. Surf. Sci. 94&95 (1996) 370.

[16] P. Pareige, PhD thesis, Rouen University (1994).

[17] P. Auger, P. Pareige, M. Akamatsu, D. Blavette, J. Nucl. Mater. 225 (1995) 225.

[18] M.A. Sokolov, S. Spooner, G.R. Odette, B.D. Wirth, G.E. Lucas, SANS Study of High-Copper RPV Welds in Irradiated and Annealed Conditions, Effects of Radiation on Materials: 18th Int. Symp. ASTM STP 1325 (American Society for Testing Materials, Philadelphia, PA) to be published.

[19] C.A. English, W.J. Phythian, J.T. Buswell, J.R. Hawthorne, P.H.N. Ray, in: R.E. Stoller, A.S. Kumar, D.S. Gelles eds., Effects of Radiation on Materials: 15th Int. Symp., ASTM STP 1125 (American Society for Testing and Materials, Philadelphia, PA, 1992) p. 93.

[20] F. Frisius, R. Kampmann, R. Wagner, P.A. Beaven, Proc. 2nd Int. Symp. on Environmental Degradation of Materials in Nuclear Power Systems – Water Reactors, Monterey, CA, 1985, p. 400.

[21] M.K. Miller, D.T. Hoelzer, F. Ebrahimi, J.R. Hawthorne, M.G. Burke, J. Phys. (Paris) 48C6 (1987) 423.

[22] M.G. Burke, M.K. Miller, J. Phys. (Paris) 49C6 (1988) 283.

[23] T.J. Griesbach, W.L. Server, in: Radiation Embrittlement of Nuclear Reactor Pressure Vessel Steels: An International Review, ASTM STP 1170, ed. L.E. Steele (American Society for Testing and Materials, Philadelphia, PA, 1993) p. 30.

[24] S.R. Goodman, S.S. Brenner, J.R. Low, Metall. Trans. 4 (1973) 2363.

[25] P. Pareige, K.F. Russell, M.K. Miller, Appl. Surf. Sci. 94&95 (1996) 362.